CHAPTER 16

FUNCTIONAL MEASUREMENTS IN NUCLEAR MEDICINE

M.J. MYERS
Institute of Clinical Sciences,
Imperial College London,
London, United Kingdom

16.1. INTRODUCTION

The strength of nuclear medicine lies in using the tracer method to acquire information about how an organ is or is not functioning as it should. This modality, therefore, focuses on physiological organ function for diagnoses and not on anatomical information such as X ray computed tomography (CT) or magnetic resonance imaging.

The three aspects involved in the process are: (i) choice of radioactive tracer, (ii) method of detection of the emissions from the tracer, and (iii) analysis of the results of the detection. The radioactive tracers on which nuclear medicine (or molecular imaging as it is increasingly being called) is based are designed to participate in or 'trace' a chosen function of the body. Their distribution is then found by detecting and locating the emissions, usually γ photons, of the radioactive tracer. The tracer may be involved in a metabolic process, such as iodine in the thyroid, or it may take part in a physiological process because of its physical make-up, such as macroaggregate of albumin (MAA) in the lungs.

A number of methods of detection can be used. One is imaging with a gamma camera or positron emission tomography (PET) scanner in a number of modes: static (showing an accumulated or integrated function), dynamic (showing the variation of the function with time), whole body and tomographic (single photon emission computed tomography (SPECT) and PET analysis). Another is simple counting over areas of the body which can also be static or dynamic. Yet another is through laboratory analysis of blood samples. Imaging often provides a rough anatomical distribution of the function but, more importantly, a quantitative idea of the extent of the function in the whole functional unit or in component parts such as the right and left kidney. The anatomical picture has little of the detail of the other modalities but may be a more direct tool in assessing pathology since it provides primary information rather than displaying the anatomical consequences of pathology such as changes in density. The images created can

be directly related to the uptake of the radiopharmaceutical, either in terms of counts or, with more sophisticated processing, with activity in becquerels. As parametric images, they can also represent a parameter such as the distribution of the ratio of ventilation V to perfusion Q, the V:Q ratio. The results can be acquired and displayed as 2-, 3- or 4-D images with time as the last dimension. In addition, because of the unique property of nuclear medicine to be able to detect specific radionuclides with different energy γ emissions, a number of functions can be followed simultaneously. Thus, the ventilation of the lung traced by ^{81m}Kr, a 190 keV γ emitter, can be investigated at the same time as the perfusion of the lung traced by the 140 keV γ emitting ^{99m}Tc-MAA.

16.2. NON-IMAGING MEASUREMENTS

'Non-imaging' measurements refer to the analysis of data from radionuclide procedures that are not derived from interpreting normal and pathological patterns of uptake of tracer in images from gamma cameras and PET scanners. Images may be used for non-imaging measurements but only to provide regions of interest (ROIs) for subsequent quantification of function. A common example of this is in the investigation of glomerular filtration in the kidney using a tracer such as ^{51}Cr-EDTA which can be measured from timed blood samples without using images for information about morphological changes.

16.2.1. Renal function measurements

16.2.1.1. General discussion

Renal haemodynamic functions can be divided into measurements of renal blood flow and glomerular filtration. The first depends on the supply of blood to the cortical and extramedullary nephrons which are the functional unit of the kidney. The second class of function depends on the transfer of fluids across the glomerulus. A number of radioactive tracers may be used depending on the function to be studied, the most common being ^{99m}Tc labelled diethylenetriaminepentaacetic acid (DTPA), dimercaptosuccinic acid (DMSA) and mercaptoacetyltriglycine (MAG3).

16.2.1.2. Glomerular filtration rate plasma clearance

Calculation of glomerular filtration rate (GFR) is used, for example, in the general assessment of renal function and the monitoring of renal function in patients undergoing therapy with nephritic drugs. Radioisotope measurements

depend on the assessment of plasma clearance with time as seen with blood sampling of a tracer that is handled exclusively by glomerular filtration and does not enter blood cells. The most common radiopharmaceutical used is ^{51}Cr-EDTA, though ^{99m}Tc-DTPA and ^{125}I-iodothalamate are also seen.

GFR is obtained by constructing the clearance curve from one or a series of timed measurements of plasma activity. In the multi-sample method, the expected multi-exponential curve is defined accurately with samples taken at 10, 20 and 30 min, and 2, 3 and 4 h, or approximated with samples taken at about 2 and 4 h or even at only one time point between 2 and 4 h. As taking multiple samples over a period of hours may be impractical, further simplification of the process to the taking of a single sample is attractive. An empirical relationship between the apparent volume of distribution and the GFR has been derived and validated to allow this at a less precise but acceptable accuracy.

The object of the measurements is to construct the total area under the plasma clearance curve. It is sufficient for accuracy to assume a bi-exponential curve with a fast and slow component between times of 10 min and 4 h, ignoring any initial very fast components. The zero time intercepts and rate constants for the fast and slow components are C_{10} and α, and C_{20} and β, respectively. The equation for GFR is:

$$\text{GFR} = \frac{\text{injected activity}}{\text{total area under plasma clearance curve}} = \frac{Q_0}{A} = \frac{Q_0}{\frac{C_{10}}{\alpha} + \frac{C_{20}}{\beta}} \tag{16.1}$$

where

injected activity has units of megabecquerels (MBq);
C_{10} and C_{20} are in count rates that are converted into megabecquerels per millilitre (MBq/mL);

and α and β have units of min^{-1}, so that the GFR has units of millilitres per minute (mL/min).

As the contribution to the whole area from the fast component is relatively small and can be approximated without too much loss of accuracy, the equation can be simplified to:

$$\text{GFR} = \frac{Q_0}{C_{20}/\beta} \tag{16.2}$$

This produces an estimate of GFR that is obviously too small, though with poor renal function the approximation has less of an effect. A correction factor to convert the approximate GFR to the 'true' GFR can be used. Although this correction factor depends on the renal function, a figure of 1.15 can be used in most cases.

GFR will vary with body size and is conventionally normalized to a standard body surface area of 1.73 m^2, though other normalization variables such as the extracellular fluid volume have been suggested. The calculation for GFR requires measurement of the activity injected into the patient as well as the activity in the post-injection syringe, in a standard and in the blood samples. A number of methods are available in practice. These are based on the difference in weights of the pre- and post-injection syringe or on measurement of a fixed volume in a dose calibrator or on known dilutions. The counts recorded by the well counter measuring the small activities in the blood samples also have to be calibrated in terms of megabecquerels per count rate (MBq/count rate).

16.2.1.3. Effective renal plasma flow measurements

Renal plasma flow, often referred to as renal blood flow, has been investigated in the past using ^{131}I or ^{123}I labelled ortho-iodohippurate (hippuran) or para-amino hippurate (PAH).

Hippuran is almost completely excreted by the renal tubules and extracted on its first pass through the renal capillary system. As the extraction is not quite 100%, the renal function measured is called the effective renal plasma flow (ERPF). A modern variation is to use the ^{99m}Tc labelled tubular agent MAG3 as the ^{99m}Tc label is more available than ^{123}I. However, the extraction fraction of MAG3 at below 50% is inferior to that of hippuran, so the measurements of ERPF are simply estimates.

The ERPF measurement is very much the same as that of GFR in that a known activity of the radiopharmaceutical is injected and blood samples are taken at intervals. The timing of the intervals is, however, earlier than for GFR and occurs at 5 min intervals and then at 30, 50, 70 and 90 min. The resulting two-exponential time–activity curve is plotted from which the function is given as:

$$\mathrm{ERPF} = \frac{Q_0}{\frac{C_{10}}{\alpha} + \frac{C_{20}}{\beta}} \tag{16.3}$$

using the symbols for GFR as above.

16.2.2. ^{14}C breath tests

The ^{14}C urea breath test is used for detecting *Helicobacter pylori* infection in cases of, for example, patients with duodenal and other ulcers following and monitoring anti-*H. pylori* treatment. The test is based on the finding that the bacterium *H. pylori* produces the enzyme urease in the stomach. As urease is not normally found in that organ, its occurrence can, therefore, denote the existence of *H. pylori* infection. The activity of ^{14}C used in the test is very small, about 37 kBq, and the effective dose for this is also low, at less than 3 μSv.

To carry out the test, ^{14}C urea is administered orally in the form of a capsule. The urease in the stomach converts the urea to ammonia and ^{14}C carbon dioxide which is exhaled and can be detected in breath samples using a liquid scintillation counter. The counter can measure minute quantities of the β emitting ^{14}C. One or two samples are usually collected after 10–30 min using a straw and balloon technique. Also counted are a known standard sample and a representative background sample. Counting is done either locally or by sending the samples to a specialized laboratory. The net disintegrations per minute (dpm) registered by the counter are compared with standard values to assess the degree of infection. dpm is given by:

$$\text{dpm} = \frac{(S-B)\times S_t}{(S_t-B)} \tag{16.4}$$

where

S is sample counts per minute;
B is blank counts per minute;

and S_t is standard counts per minute.

A non-radioactive test employing ^{13}C in place of ^{14}C is also used. Carbon-13 is measured by (non-radio)isotope ratio mass spectrometry. For ^{13}C, a baseline sample is required before the capsule is swallowed to compare with the post-capsule sample.

16.3. IMAGING MEASUREMENTS

These include static image acquisition and analysis for quantitative assessment of uptake, e.g. thyroid uptake measurement with organ delineation and background subtraction. Furthermore, time–activity curves can be derived

from dynamic 2-D imaging and quantitative parameters assessed from images, e.g. renal function, gastric function, gall bladder emptying, gastrointestinal transit and oesophageal transit. Time–activity curves can also be derived from dynamic 3-D imaging with quantitative parameters assessed from physiologically triggered images, such as cardiac ejection fraction measurement.

16.3.1. Thyroid

Measurement of thyroid function is one of the oldest techniques in nuclear medicine, though the original radioisotope used, ^{131}I, has been replaced by ^{99m}Tc and ^{123}I, and the collimated sodium iodide crystal uptake probe has almost exclusively been replaced by the gamma camera.

Tests on the thyroid consist of both imaging the morphology of the organ and assessing its 'uptake'. Uptake consists of measuring the activity taken up by the gland of an ingested or intravenously administered activity of radioactive iodine or intravenously administered ^{99m}Tc-pertechnetate. The uptake mechanisms are different for the two radioisotopes. Iodine is both trapped and organified by thyroid follicular cells, a process more like the true thyroid function, whereas the pertechnetate is simply trapped.

The tests allow assessment of functionality of thyroid lesions and nodules, and investigations of thyroiditis and ectopic tissue. They can confirm a diagnosis of an excess of circulating thyroid hormones, as in Graves' disease and toxic nodular goitre, and lead to a more quantitative approach to treatment of hyperthyroidism with ^{131}I.

Uptake of tumours secondary to thyroid cancer that have disseminated through the body following surgery may also be assessed. In this case, whole body images are made using ^{131}I and a scanning gamma camera. The tumours can be located and, in some cases, a quantitative measurement of uptake made, thus allowing the effectiveness of treatment to be monitored.

The choice of radiopharmaceutical used can be dictated by the availability and cost of the preferred isotope ^{123}I and ^{99m}Tc. Each is suitable for use with a gamma camera. Iodine-123 has a half-life of 13 h and a γ emission of 160 keV. Technetium-99m has a half-life of 6 h and an energy of 140 keV. However, the cyclotron produced ^{123}I is not readily available and is expensive, while ^{99m}Tc-pertechnetate is readily available from the standard hospital molybdenum generator. The timing of the uptake of the two isotopes is also different. While iodine uptake is usually performed 18–24 h after injection or 2–6 h after ingestion, ^{99m}Tc is measured after 20 min.

Uptake measurement with a scintillation probe involves counting over the neck, over a 'thyroid phantom' and over the thigh of the patient to simulate counts in the neck that do not arise from the thyroid. The thyroid phantom (standardized

by, for example, the IAEA) consists of a small source of known activity in a plastic cylinder offering the same attenuation as a neck. This acts as the standard. Counts are obtained at a distance of about 25 cm from the collimator face to offset any inverse square errors due to different locations of the thyroid. The percentage uptake U is then calculated from the formula:

$$U = \frac{N - T}{C_a} \times 100 \tag{16.5}$$

where

N is the counts in the neck;
T is the counts in the thigh;

and C_a is the administered counts corrected for background.

The administered counts can be measured directly with an isotope calibrator before the test or can be related to the activity in the thyroid phantom. Corrections for decay are made throughout.

Similar measurements can be made with the gamma camera in place of the probe, except that corrections for neck uptake can be made using ROIs over the delineated thyroid and regions away from the gland. The camera can be fitted with a pinhole collimator in order to provide a degree of magnification, although the image is somewhat distorted and is subject to distance errors, in which case a fixed distance (perhaps employing a spacer) is used. Images obtained with a parallel-hole collimator may appear smaller but are not prone to distance effects, though subject to the same attenuation. Anterior views are generally enough but a lateral view may also be used to locate ectopic tissue.

Quantification of the uptake is achieved in two ways. By calibrating the camera with a known activity in a suitable phantom, the activity injected into the patient can be measured, or by measuring the injection directly in the syringe before administration. Each will yield the sensitivity of the camera in terms of counts per megabecquerel and allow the activities seen in the thyroid glands and background to be calculated. The process is often an automatic one performed by the camera computer software that delineates the outlines of the thyroid lobe(s) and establishes a suitable background region used to correct for the presence of activity in tissue overlying and underlying the thyroid tissue correction. It is important that a local normal range is established and that the calibration of the camera in terms of counts per megabecquerel is subject to a quality assurance programme.

A simple check on the quantification is to perform the test on a syringe of activity as if the syringe is the thyroid gland, i.e. imaging the syringe as the activity to be injected and re-imaging it as the activity taken up by the thyroid. An 'uptake' of 100% would be expected.

16.3.2. Renal function

16.3.2.1. General discussion

The study of renal function has been a mainstay of nuclear medicine for many decades and is an established efficient technique for, among other functions, assessing renal perfusion, quantifying divided or individual kidney function, and studying output efficiency and obstruction.

Two aspects of renal function are exploited: (i) glomerular filtration, i.e. the transfer of fluids across the glomerulus, investigated by measuring the clearance of ^{99m}Tc-DTPA ('pentetate'); and (ii) tubular secretion, investigated by measuring the clearance of ^{99m}Tc-MAG3 ('tiatide').

16.3.2.2. Renal function measurements

The basis of measurements of most renal functions is time–activity curves obtained by imaging the kidneys using a gamma camera. Views are obtained at different times and over different periods after administration of one of a number of radiotracers and often after some intervention. The result is usually a curve, called a 'renogram', showing the rise and fall of counts in each kidney. This curve is corrected for non-renal background counts using computer software, a feature lacking in old counting methods using probes. Figure 16.1 shows a series of images obtained after administration of ^{99m}Tc-MAG3 (left), the ROIs drawn over the two kidneys as well as the background region (top right), and the renogram curves for the right kidney (RK) and left kidney (LK) (bottom right). The analysis programmes, supported by commercial software providers, allow the calculation of a number of renal function parameters, including relative perfusion, relative function, mean and minimum transit times, and outflow efficiency.

There is an overabundance of different methods of analysis of the curves to create a plethora of indices of function, some relying on the definition of aspects of the renograms that have little basis in renal physiology. It is, therefore, prudent to understand what is happening to the tracer as it traverses the kidneys, and how it appears in the images and renogram. In fact, after adjustment for the contributions of activity in the renal vasculature, the corrected curve displaying a relatively fast rise and subsequent slower fall in activity can be described by two distinct phases. The first spans the time of injection to the end of the minimum

transit time when the kidney contains the sum of all of the tracer extracted from the blood and has, therefore, been termed the sum phase. The second starts at the end of the first and reflects the net activity left after loss from the kidney and has been called the difference phase. Other terms such as 'vascular spike' and 'secretory phase' may not reflect purely renal function and are, therefore, not very helpful.

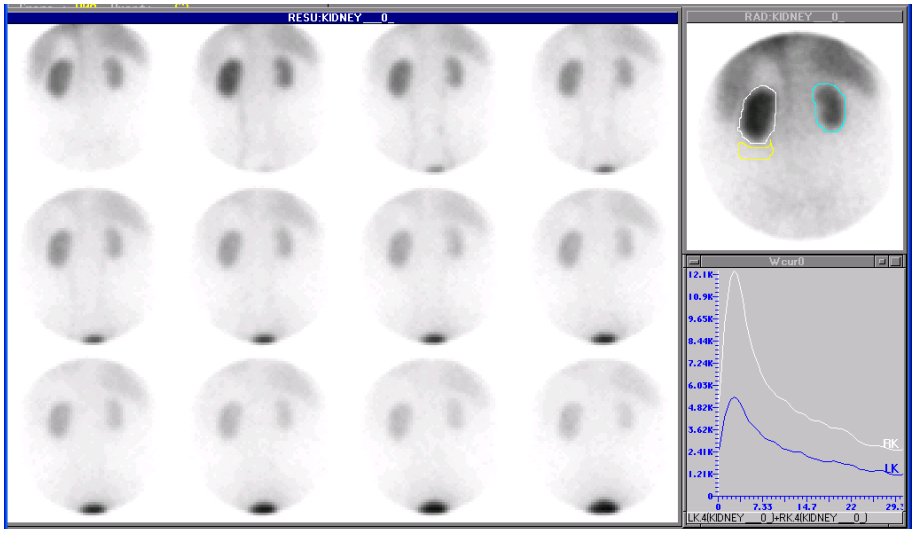

FIG. 16.1. Dynamic renal flow study after administration of ^{99m}Tc-MAG3 (left), regions of interest drawn over the kidneys and background (top right), and corresponding renogram curves for the right kidney (RK) and left kidney (LK) (bottom right).

What is helpful is often a quantitative comparison of the two kidneys with derivation of a relative function. This may be calculated from Patlak plots or from the uptake slope or the integral of the renogram curves. The programme can calculate the relative perfusion and function from the retention functions. The outflow curves for both kidneys and the value of the outflow at any selected time can also be displayed. In the case of assessment of kidney transplants, other aspects can be used to calculate relevant parameters.

A number of radioactive tracers may be used, depending on the function to be studied. These functions are measured by ^{99m}Tc labelled DTPA, DMSA and MAG3. Renal blood flow (or renal plasma flow) has been measured from clearance of hippurate from the plasma.

16.3.3. Lung function

The functions of the lung that are most investigated using nuclear medicine techniques are regional ventilation and pulmonary blood flow or perfusion, leading to studies of the ventilation perfusion ratio. Other studies cover intrapulmonary vascular shunting, pulmonary granulocyte kinetics and lung tissue permeability.

Lung air flow or ventilation imaging is carried out either with a gas such as ^{81m}Kr (a 13 s half-life radioisotope generated from ^{81}Rb that has a 4.6 h half-life) or with an aerosol containing particles of sizes between 0.1 and 2 μm, typically ^{99m}Tc-DTPA or carbon particles ('Technegas'). The use of ^{133}Xe gas has largely been discontinued.

Lung blood flow or perfusion imaging is carried out with macroaggregates or microspheres of denatured human serum albumin (MAA). These particles of average size 20–40 μm are larger than the lung capillaries and are trapped in the capillary bed, distributing according to the blood flow to a region. Their main use is to image pulmonary vascular disease, in particular, pulmonary embolism.

The two techniques are often employed together, either simultaneously (e.g. ^{81}Kr and ^{99m}Tc-MAA) or sequentially (^{99m}Tc aerosol and ^{99m}Tc-MAA). The presence or absence of ventilation and/or perfusion is of clinical significance.

16.3.4. Gastric function

Nuclear medicine allows a full, non-invasive and quantitative assessment of the way the oesophagus moves both solid and liquid meals to the stomach, how the stomach handles these meals and how they transit through the gastrointestinal tract.

16.3.4.1. Stomach emptying of solid and liquid meals

As the choice of both solid and liquid test meals determines the standard values used as criteria for evaluating the function, a 'standard meal' has been agreed. Solid meals are based on preparations including eggs (into which ^{99m}Tc sulphur colloid has been mixed), toast and water.

Anterior and posterior dynamic images are obtained at suitable intervals of time following ingestion of the meal and are repeated for the same positioning at hourly intervals for up to 4 h. The two views are obtained simultaneously or sequentially, depending on the availability of a dual or single headed gamma camera. The reason for the two view approach is to obtain a geometric mean of the activity in the field of view that accounts for the movement of activity

between the anterior and posterior surfaces of the body. Relying on a simple anterior view leads to artefacts due to differential attenuation of the ^{99m}Tc γ rays.

The data are analysed by drawing ROIs around the organs of interest (stomach and parts of the gastrointestinal tract) and creating a decay corrected time–activity curve. An assessment of the gastric emptying function is made from standard values. An alternative way of expressing the result is through the half-emptying time.

16.3.4.2. Analysis of colonic transit

Colonic transport analysis can be performed using ^{111}In labelled non-absorbable material, such as DTPA or polystyrene micropellets administered orally. Indium-111 is chosen rather than the more accessible ^{99m}Tc because of its longer half-life (2.7 d) and the possibility of imaging over a longer time since images are taken at, for example, 6, 24, 48 and 72 h.

As with the stomach procedures, a geometric mean parametric image of anterior and posterior views may be used in the quantification, if this facility is available in the nuclear medicine software. A geometric centre of the activity (also called centre of mass) may be tracked over time by defining particular segments in the colon, perhaps 5–11 in number (e.g the ascending, transverse, descending, rectosigmoid and excreted stool), multiplying the individual segment counts by weighting factors from 1 to 5, respectively, and summing the resulting numbers. In addition to time–activity curves for the individual segments, the rate of movement of the geometric centre as a function of time can be assessed by plotting this as a time position profile. A colonic half-clearance time may be calculated and compared with historical normal control values of colonic transport.

16.3.4.3. Oesophageal transit

This function is studied by imaging the transit of a bolus of radiolabelled non-metabolized material such as ^{99m}Tc sulphur colloid. Either the whole oesophagus may be included in an ROI and a time–activity curve generated for the whole organ, or a special display may be generated, whereby the counts in successive regions of the oesophagus are displayed on a 2-D space–time map called a condensed image. The counts in the regions are displayed in the y direction as colour or grey scale intensities corresponding to the count rate against time along the x axis (Fig. 16.2). The result is a pictorial idea of the movement of the bolus down the oesophagus.

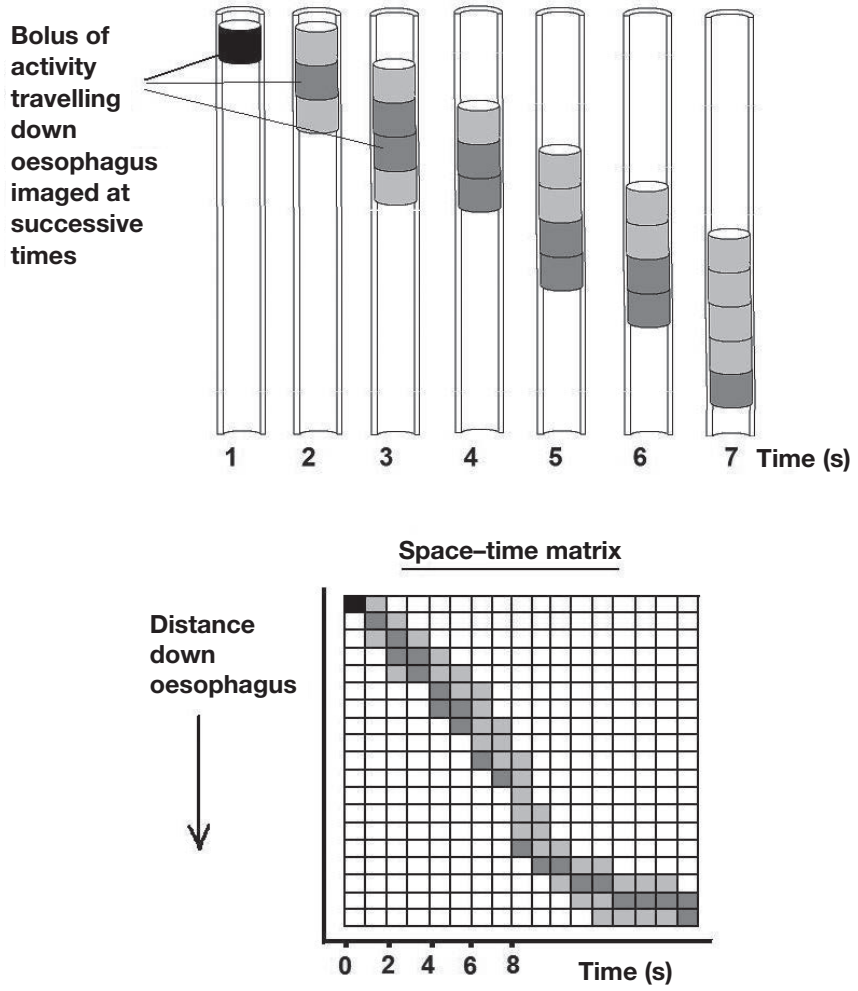

FIG. 16.2. Oesophageal transit is imaged as a space–time matrix. As the bolus of radioactivity passes down the oesophagus, the counts from successive regions of interest, represented on a grey scale, are placed in consecutive positions in the matrix in the appropriate time slot. A normal transit will be shown as a movement of the bolus down and to the right in the matrix. Retrograde peristalsis will be shown as a movement to the right and upwards.

16.3.4.4. Gall bladder ejection function

The gall bladder is investigated using hydroxy iminodiacetic acid labelled with ^{99m}Tc. This is injected and can be imaged using a gamma camera after excretion by the liver into the bile and as it passes through the gall bladder and

bile ducts. The gall bladder is then made to contract and empty by injecting a hormone called cholecystokinin and the imaging of the gall bladder continued, the whole test taking between 1 and 2 h. The amount of the radiolabel that leaves the gall bladder is assessed by the difference in counts in the ROI over the emptied gall bladder divided by the counts from the ROI over the full gall bladder. Expressed as a percentage, this gives the ejection fraction. An ejection fraction above 50% is considered as normal and an ejection fraction below about 35% as abnormal, suggesting, for example, chronic acalculous cholecystitis.

16.3.5. Cardiac function

16.3.5.1. General discussion

The two main classes of cardiac function are blood flow in the myocardium and in the blood pool and ventricles. Images are acquired in both planar and tomographic modes, and the data may be acquired dynamically over sequential time periods or as a gated study triggered by the electrocardiogram (ECG), or as part of a first-pass study. The information is presented on a global or regional basis as conventional or parametric images, or as curves from which quantitative parameters may be derived. A range of pharmaceutical agents labelled with single and positron emitting isotopes are used.

Cardiac functions that may be investigated with nuclear medicine techniques run into many dozens, though relatively few are covered by standard clinical practice and some are confined to research. A list of cardiac functions would, therefore, include myocardial perfusion, myocardial metabolism of glucose and fatty acids, myocardial receptors, left ventricular ejection fraction, first-pass shunt analysis, wall motion and thickness, stroke volumes, cardiac output and its fractionation, circulation times, systolic emptying rate, diastolic filling rate, time to peak filling or emptying rate, and regional oxygen utilization.

Despite the usefulness of nuclear cardiology procedures, a worldwide survey has shown a wide variation in their use and availability. There is a high application rate in the United States of America (where cardiology accounts for about half of nuclear medicine procedures) and Canada, less in western Europe and Japan, and low application elsewhere such as in the Russian Federation, Asia and some parts of South America. One reason for this pattern of use may be the degree of access to training for physicians. Another reason may be that gated SPECT imaging and analysis requires a high level of instrumentation and software.

However, the procedures that can be carried out in any particular department will depend very much on the nuclear medicine software provided by the supplier of the gamma camera or from a specialized nuclear software supplier.

A commercial suite of programmes will usually only offer a limited selection of functional analysis. Typically, these include blood pool gated planar or SPECT analysis for ventricular volumes and ejection fractions, and cardiac perfusion analysis of gated SPECT images acquired under stress/rest conditions. The sophistication of the programmes may also be limited in the extent of automation of the preparation of cardiac images and their analysis. Whereas in the earlier days of nuclear medicine a programmer could be asked to tailor programmes to suit the need of the practitioner, and a high level language or macro-language might be provided to allow this, the fashion nowadays is for a fixed set of programmes dictated by the commercial supplier to satisfy a perceived general need. A typical omission might, therefore, be list-mode data acquisition with the consequent inability to trigger on selected parts of the ECG to omit ectopic heart beats.

In addition to the aspect of the software provided is the choice of radiopharmaceutical available. A wide choice is theoretically possible, depending on the particular function to be explored. Thus, for example, myocardial receptors can be investigated using ^{123}I-MIBG (metaiodobenzylguanidine) or ^{11}C-hydroxyephedrine, myocardial glucose using ^{18}F-FDG (fluorodeoxyglucose) and fatty acid metabolism using ^{123}I-heptadecanoic acid or BMIPP (β-methyl-p-iodophenylpentadecanoic acid). SPECT techniques use ^{201}Tl, ^{99m}Tc-sestamibi and other perfusion agents. PET viability studies can employ ^{13}N-ammonia, ^{18}F-FDG and ^{11}C-acetate.

In terms of which gamma camera radiopharmaceutical is best to use, there may be limitations in the availability or the licensing of a ^{201}Tl or a ^{99m}Tc product. As far as PET imaging goes, it is obvious that the non-research use of short lived positron emitters such as ^{11}C or ^{13}N that would be useful in the study of myocardial function would depend on the proximity of a cyclotron as well as the funding to allow the production of the labelled products. It would also presuppose the existence of an expensive PET/CT scanner for the procedures.

16.3.5.2. First-pass angiography

First-pass studies typically involve the acquisition of about 2000 frames of data with a duration of about 50 ms following the bolus injection of autologous red blood cells labelled in vivo or in vitro with ^{99m}Tc as they pass through the right ventricle for the first time. A time–activity curve derived from an ROI over the ventricle shows a curve that rises to a peak and then falls off, the curve also showing a saw tooth pattern corresponding to the filling and emptying of the left ventricle during the cardiac cycle. The first-pass curve is illustrated in Fig. 16.3(a) alongside the volume curve in Fig. 16.3(b), also used to derive the ejection fraction obtained from a multiple-gated acquisition (MUGA) study.

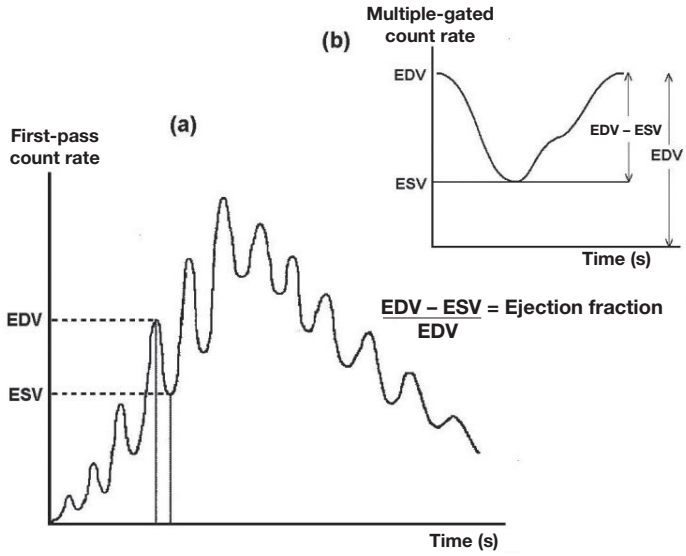

FIG. 16.3. Curves obtained from (a) first-pass angiography and (b) a multiple-gated acquisition study, showing how end diastolic volume (EDV) and end systolic volume (ESV), used to determine ejection fraction, are represented in each technique.

By suitable positioning of the gamma camera in the right anterior oblique view, this saw tooth can be used as an estimate of ejection fraction in the right ventricle, a parameter that is only amenable to analysis in the first pass before uptake in adjoining structures. The ejection fraction is derived from the ratio of the peak of any saw tooth (the end diastolic volume (EDV)) minus the value of the next trough (the end systolic volume (ESV)) to the EDV. The ejection fraction for the left ventricle would be assessed from the curve obtained by viewing in the left anterior oblique position. Although this parameter is more reliably obtained from a MUGA study, the first-pass procedure is much quicker and may be suitable for patients who cannot tolerate the much longer MUGA study. First-pass kinetics also provide a measure of left to right cardiac shunts (where some activity goes from the left ventricle through a septal defect to the right ventricle and, thus, recirculates between the heart and the lungs) and the pulmonary systemic flow ratio (Q_p:Q_s), as well as systolic emptying and diastolic filling rates and ventricular volumes.

16.3.5.3. The multiple-gated acquisition scan

The MUGA scan traces heart muscle activity from the distribution of the administered radiopharmaceutical, allowing the calculation of the left ventricular

ejection fraction and demonstrating myocardial wall motion. It may be obtained while the patient is at rest and after physically or pharmacologically induced stress.

The same radiopharmaceutical preparation is used as for the first-pass study and a bolus is injected. The gamma camera views the patient in the left anterior oblique position so as to best separate the projections of the two ventricles. Dynamic images of the left ventricle in a beating heart are acquired at the same time as the ECG and the results stored. A trigger ('gating signal') corresponding to the R-wave marks the start of each heart cycle and the start of each sequence of images. The time period between successive R-waves (R–R interval) is divided into time intervals and the beat by beat left ventricular images corresponding to each time interval are each integrated into a single combined 'gated' image that provides a stop motion image of the heart at intervals in its cycle. As any one frame would not have enough data to provide sufficient counts and would, therefore, be statistically unreliable, many frames at the same interval are superimposed on each other. The signal for the start of each sequence is derived from an ECG monitor connected to the patient that provides a short electronic pulse as it detects the peak of an R-wave. Usually, about 32 equally time-spaced frames ('multiple gates') are used and these are defined between each R–R interval. Beats within 10% of the mean length are accepted. The result is a series of images of the heart at end diastole and at end systole, and at stages in between (Fig. 16.4).

The image at end diastole when the heart has filled with blood contains the maximum number of counts, and the end systolic image the least number. A direct relationship is made between the number of counts in a region of the ventricle and its volume.

For each frame, the computer, starting with an initial rough outline provided by the operator, defines the boundary of the left ventricle. Depending on the computer programme used, a different method of edge detection may be employed. This may be based on an isocount contour or on a maximum slope normal to the edge. As there is interference with the ventricular image from activity seen in pulmonary blood, the computer will also define a suitable background ROI close to the wall and correct the ventricular image at each stage. The plot of the counts in the ventricular region against time forms the volume curve that starts with the EDV, falls to the ESV level and rises again. The ejection fraction is calculated as before from the standard formula:

$$\mathrm{EF} = \frac{\mathrm{EDV} - \mathrm{ESV}}{\mathrm{EDV}} \tag{16.6}$$

Simple differentiation of the volume curve provides indices of the ventricular filling and emptying rates. Indeed, if the cardiac output is known, the rates can be quantified in terms of millilitres per minute. Other information can be obtained from phase/amplitude analysis of the sequence of images.

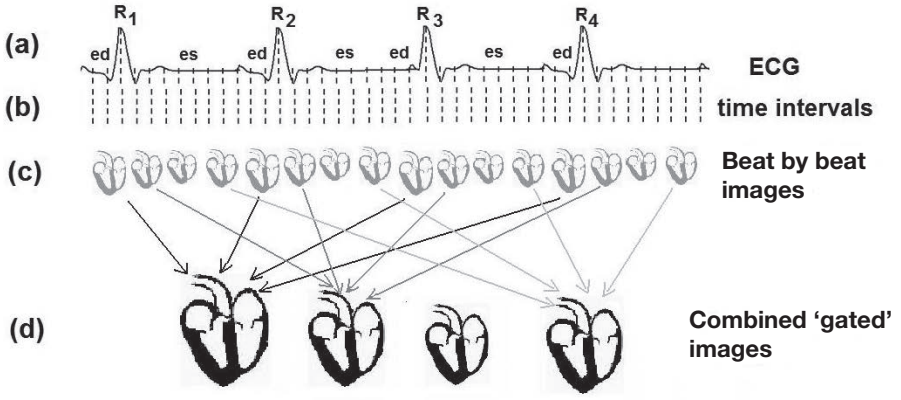

FIG. 16.4. The multiple-gated acquisition scan. The sequence of these gated images shows the heart cycle with higher counts and better statistics than the individual images, allowing better interpretation of the data than in Fig. 16.3(b).

16.3.5.4. Myocardial perfusion imaging

Myocardial perfusion imaging allows a regional assessment of blood flow to the heart and demonstrates areas of ischaemic myocardium where the blood flow is diminished when the patient undergoes a stress test.

Imaging follows administration of specific radiopharmaceuticals such as ^{201}Tl-chloride, ^{99m}Tc-tetrofosmin or ^{99m}Tc-sestamibi after the patient has been subjected to physical exercise or, if this is not suitable, to pharmacological stress with vasodilators to raise the heart rate and stimulate the myocardium. This induces a difference of uptake of radiolabel between normal and ischaemic myocardial tissue that can be imaged and localized after planar and/or ECG gated tomographic imaging. It is also possible to use positron emitting radiopharmaceuticals such as the cyclotron produced 10 min half-life ^{13}N-ammonia and generator produced 75 s half-life ^{82}Rb, but there are the usual limitations on applicability of PET, such as availability of the product or imaging system.

Once a stable ECG pattern is observed, the patient is imaged using a gamma camera operating in SPECT mode. ECG gating is applied throughout and produces sets of 16 images at each acquisition angle. The stress images and their

analysis may be compared with similar ones obtained with the patient at rest. A number of protocols involving different times of examination and different administrations of radioactivity have been devised to carry out the stress/rest examinations in one rather than two days, given the potential long washout periods involved. Imaging can be performed 'early' (at about 15 min) following injection of ^{201}Tl or ^{99m}Tc-sestamibi at rest or after the stress test and/or 'delayed' (after 1–4 h or after 24 h) after injection at rest or under stress of the longer lived ^{201}Tl. These protocols give rise to different types of image. In general, the imaging properties of ^{99m}Tc give superior images, though ^{201}Tl is superior from a physiological viewpoint as it is a better potassium analogue.

Conventional cardiac SPECT imaging may be carried out with a single or double headed gamma camera using circular or elliptical orbits, the latter allowing closer passes over the patient and, consequently, better resolution. Attenuation correction may be performed on the emission images using an isotope or CT X ray source. However, there is still debate as to the usefulness of attenuation correction since this technique may give rise to artefacts due to mismatch of the emission and transmission images on the fused images.

16.3.5.5. Technical aspects of SPECT and PET imaging

Thallium is not an ideal gamma camera imaging radionuclide, as it emits rather low energy characteristic X rays between 69 and 80 keV that are easily attenuated (and, therefore, lost) in the body. The attenuation, by breasts and the chest wall, varies for the different projections around the body and gives rise to artefacts in the perfusion images if not corrected. The higher γ energy of ^{99m}Tc (140 keV) while still liable to attenuation, allows better collection of data from the heart and less variation in the attenuation. Although SPECT/CT has still not become a viable option (as has PET/CT where the two modalities have become inseparable), this would be a better option for attenuation correction than the rather cumbersome isotope attenuation correction devices that have been used in the past.

Scattering of the γ photons before detection in the camera also leads to problems in that their origin might be misplaced and loss from deeper structures occurs. Recently, software to reduce the effects of scattering by modelling its behaviour within the field of view has become available. Another source of degradation of the image quality is the loss of resolution with distance from the collimator face. Although 'high' resolution collimators are usually chosen for ^{99m}Tc imaging, the basic resolution of the camera at the level of the heart is rather poor. Again, software techniques to model this behaviour and correct for it have become available.

Gamma camera images, unlike X ray ones, are always subject to lack of counts and are, therefore, prone to statistical errors. Using a double headed rather than a single headed system is, therefore, an advantage. There is still discussion on the best angle between the heads and this may vary between less than 90° and 180°. Scanning the patient with the collimator as close to the source of activity as possible also ensures the best resolution, so a non-circular orbit is usually chosen. Owing to the lack of accessible counts with ^{201}Tl (its relatively long half-life and high effective dose reducing the activity that can be administered), a general purpose collimator is used, which is more efficient but less accurate than the high resolution collimator used with ^{99m}Tc.

PET imaging based on the simultaneous detection of opposed annihilation γ radiation from the original positron radiotracer is intrinsically tomographic and invariably comes with anatomical land marking and attenuation correction from the CT. It is also more sensitive and more accurate (because of its better resolution) than SPECT and uptake of the radiopharmaceuticals can be quantified absolutely. In theory, the use of ^{13}N labelled ammonia and ^{18}F-FDG can differentiate more about the state of the myocardium, its blood flow and metabolism, than the SPECT tracers.

Processing of the data starts with filtered back projection of the data using standard filters such as a Butterworth or Hanning filter with appropriate cut-off spatial frequencies and order, or an iterative reconstruction may be performed. Attenuation correction may be applied. This stage produces a set of contiguous slices parallel to the transverse axis of the patient which can be combined to populate a 3-D matrix of data. As the heart lies at an angle to this body axis, a process of reorientation is performed. From the original matrix, the data that lay parallel to the axes of the heart itself can be selected to form vertical long axis (parallel to the long axis of the left ventricle and perpendicular to the septum), horizontal long axis (parallel to the long axis of the left ventricle and to the septum) and short axis (perpendicular to the long axis of the left ventricle) slices through the myocardium of the particular patient, as shown in Figs 16.5 and 14.12.

Cardiac processing software, working on features extracted from the shape of the myocardium, allows easy automatic alignment which may also be operator guided. The reoriented sections form three sets of images that are displayed in a standard format to show, for example, the apex and heart surfaces at each stage of gating of the heart cycle (Fig. 16.4). The display may take several forms including the simultaneous display of many sections in each of the three axes both at rest and after stress, or as a moving image of the beating heart. The algorithms used to carry out this process differ with the provider of the computer software and are recognized under specific names.

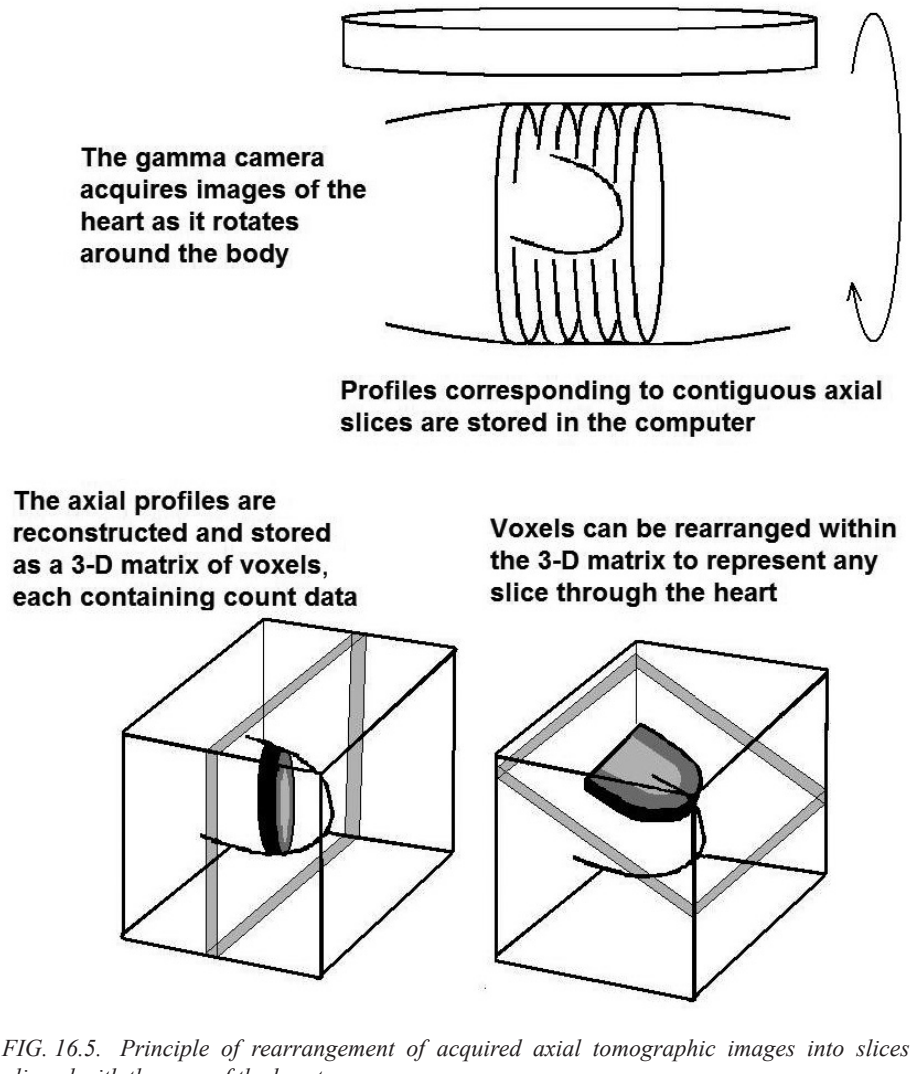

FIG. 16.5. Principle of rearrangement of acquired axial tomographic images into slices aligned with the axes of the heart.

Presentation of the slice data is often as a so-called polar diagram or bull's-eye display illustrated in Fig. 14.17. This allows the 3-D information about the myocardium, which would be difficult to interpret easily, to be depicted as a simple, 2-D, colour coded, semi-quantitative image. The process is often described as imagining the myocardial surface as the peel of half an orange which is flattened out to form the polar diagram. This is divided into accepted segments and values, and colours associated with each segment. Again, there is a variation of the exact form and mathematical basis of the polar diagram in

the commercial products available. This results in different looking maps that, although individually validated, are not directly comparable. It would, therefore, be prudent for one software package to be standardized at any one reporting centre. The results from a particular study can be compared with a reference image derived from a so-called normal database to allow a better estimation of the extent of the defects. However, it is often difficult to match the population being examined with the available validated normal data, for example, in terms of gender and ethnicity.

BIBLIOGRAPHY

PETERS, A.M., MYERS, M.J., Physiological Measurements with Radionuclides in Clinical Practice, Oxford University Press, Oxford (1998).

ZIESSMAN, H.A., O'MALLEY, J.P., THRALL, J.H., Nuclear Medicine — The Requisites, 3rd edn, Mosby-Elsevier (2006).

FURTHER READING

Recommended methods for investigating many of these functions may be found on the web sites of the American Society of Nuclear Medicine (www.snm.org), the British Nuclear Medicine Society (www.bnms.org.uk) and the International Committee for Standardization in Haematology (http://www.islh.org/web/published-standards.php).